Optical properties and Fermi-surface nesting in superconducting oxides

J. Ruvalds and A. Virosztek*
Physics Department, University of Virginia, Charlottesville, Virginia 22901
(Received 4 December 1989; revised manuscript received 25 July 1990)

Fermi-surface nesting is found to modify the electron-electron scattering and therefore yields an unusual variation of the optical reflectivity. At long wavelengths a Drude form of the dielectric function is derived with a relaxation rate for a nested Fermi liquid (NFL) that is linear in frequency for $\omega > T$. The corresponding Drude mass is also frequency and temperature dependent. Remarkably good fits to the reflectivity of $YBa_2Cu_3O_7$, $Bi_2Sr_2CaCu_2O_8$, and $La_{2-x}Sr_xCuO_4$ are achieved using an on-site Coulomb interaction of intermediate strength. The static limit for the NFL conductivity is compatible with the temperature-dependent resistivity of the high-temperature superconductors. Self-energy and vertex corrections yield a long-wavelength susceptibility that is much weaker and different in structure from the response at the nesting wave vector **Q**, and the distinctions are relevant to the Raman spectrum. In cases of imperfect nesting, a crossover to conventional Fermi-liquid behavior is possible at a temperature T^* determined by the quasiparticle orbits. Predictions for the optical response as a function of chemical composition are discussed, with attention to the anomalous resistivity of $Nd_{2-x}Ce_xCuO_4$.

I. INTRODUCTION

Infrared spectroscopy has provided valuable information on the nature of conventional superconductors such as Pb, Sn, and other metals. Classic studies[1] of the energy gap reveal the perfect reflectivity of conventional superconductors at frequencies below the energy gap and also verify other predictions of the BCS theory. At higher frequencies the reflectivity of ordinary superconductors conforms to the Drude behavior expected for good metals with a plasma frequency well in excess of the electron damping rate.

Reflectivity measurements on high-temperature superconducting oxides yield a frequency variation that is quite different from the standard Drude behavior. However, the data on single-crystal samples shows striking spectral similarities for various cuprates in the electronic response extending up to 8000 cm^{-1} ($\sim$1 eV). The unusual metallic response is restricted to the Cu-O planes. Typical data[2,3] for the reflectivity of $YBa_2Cu_3O_7$ are shown in Fig. 1, with the highest reflectivities measured to date showing a quasilinear drop in frequency over a wide ω range. The standard Drude shape of the dashed curve is at odds with the data, and attempts[2] at fits using an unrealistically large damping parameter have failed to represent the data. Experimental studies of untwinned single crystal[3] shown in Fig. 1 show remarkably small variations in the reflectivity when the light probe is polarized parallel or perpendicular to the Cu-O chains.

Previously, a variety of models[2-5] with additional "midinfrared" oscillator parameters have been used to analyze the reflectivity data, but the parameters estimated by various groups appear to lack concensus.

In view of the unusual reflectivity spectra shown in Fig. 1, extensions of the Drude behavior have been proposed to accommodate empirical frequency variations of the charge-carrier lifetime $\tau(\omega)$ and effective mass $m^*(\omega)$, which result in a modified dielectric function of the form

$$\epsilon = 1 - \frac{\omega_{pl}^2}{\omega[\omega m^*(\omega)/m_0 + i/\tau(\omega)]} , \quad (1)$$

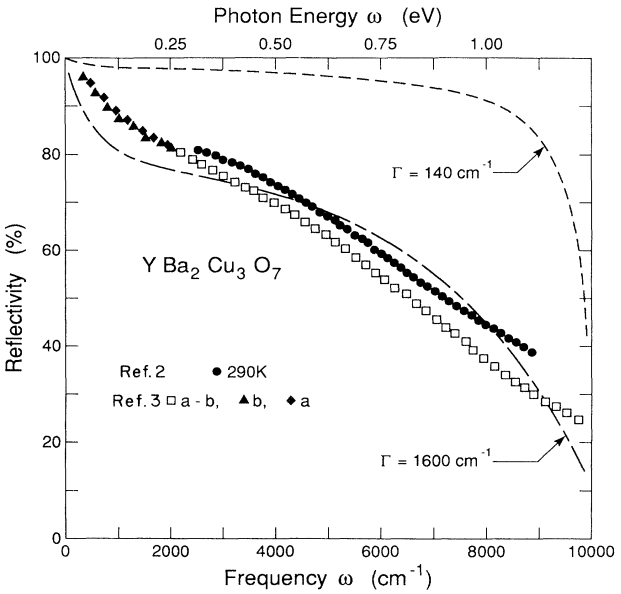

FIG. 1. Reflectivity of $YBa_2Cu_3O_7$ single crystals. The dots are from the Princeton data of Ref. 2. Squares show the IBM data for the *a-b* plane response from Ref. 3, and their most recent results on untwinned crystals are shown by triangles for the *b*-axis polarization, and crosses refer to polarization along the *a* axis. Both sets of experimental points show a quasilinear decrease with frequency, in sharp contrast to the ordinary Drude behavior displayed by the dashed curve using $\omega_{pl} = 1.2$ eV and the large damping by the dot-dashed curve.

where $\omega_{\rm pl}^2=4\pi ne^2/m_0$ is the usual long-wavelength plasma frequency for a carrier concentration n and free-electron mass m_0. Analysis of the data by Thomas *et al.*[5] and Collins *et al.*[3] yields a strong frequency variation in both $m^*(\omega)$ and $\tau(\omega)$, although differences appear in part because of their independent subtractions of midinfrared Lorentzian contributions which involve other parameters. Nevertheless, it is interesting that a qualitative behavior of $\tau^{*-1}=\tau^{-1}m_0/m^*\sim k_BT+\hbar\omega$ was foreseen from the data analysis.[3]

A fundamental issue for understanding the origin of the high-temperature superconductivity is the carrier concentration n, which may be estimated from the optical data by the f-sum rule

$$\int_0^\infty \sigma_1(\omega)d\omega=\frac{\pi ne^2}{2m} , \tag{2}$$

where the conductivity

$$\sigma_1(\omega)=\frac{\omega\epsilon_2(\omega)}{4\pi} \tag{3}$$

is a very sensitive function of the lifetime $\tau(\omega)$ and the effective mass $m^*(\omega)$ which enter in the Drude dielectric function $\epsilon(\omega)$ in Eq. (1). Hence a theoretical basis for the optical response is vital to key features such as estimates of the carrier density from experimental data.

Energy-gap estimates from reflectivity studies have remained controversial despite improved sample quality and qualitatively similar data obtained by various groups.[3-5] Here, again, the frequency and temperature variation of the damping may influence the interpretation of the data.

The purpose of the present paper is to derive the correlation functions appropriate to the optical response in situation where the Fermi surface satisfies the nesting condition $E(\mathbf{k})+E(\mathbf{k}-\mathbf{Q})\simeq 0$ for the quasiparticle energy $E(\mathbf{k})$. Such a nested Fermi liquid (NFL) has recently been found[6] to yield an anomalous frequency variation to the electron (or hole) self-energy, and analogous structure is anticipated for the dielectric function. Starting with a standard Hamiltonian

$$H=\sum_{\mathbf{k},\sigma} E(\mathbf{k})c_{k\sigma}^\dagger c_{k\sigma}+U\sum_i n_{i\uparrow}n_{i\downarrow} , \tag{4}$$

where $U>0$ denotes the on-site Coulomb repulsion, $c_{k\sigma}^\dagger$ ($c_{k\sigma}$) are the creation (destruction) operators for an itinerant electron or hole within a band $E(\mathbf{k})$) of width W, a self-consistent treatment of the electron-electron scattering gives a susceptibility at the nesting wave vector $\mathbf{Q}$ in the form[6]

$$\chi''_{\rm NFL}(\mathbf{Q},\omega)=N(0)\tan^{-1}\left[\frac{1}{\alpha}\right]\tanh\left[\frac{\omega}{\gamma T}\right] , \tag{5}$$

where γ ranges from 4 in the weak-coupling ($\alpha\ll 1$) limit to π in the strong-coupling ($\alpha\gg 1$) regime. The amplitude factor is determined by the condition

$$\alpha=\bar{g}^2\tan^{-1}(1/\alpha) , \tag{6}$$

where $\bar{g}\equiv U/W$ is a dimensionless electron-electron coupling.

Providing that the electron-scattering cross section is dominated by $\chi''(\mathbf{Q},\omega)$, the corresponding electron self-energy becomes[6]

$$-\Sigma''_{\rm NFL}(\omega)=\Gamma_{\rm NFL}(\omega)=\alpha\max(\beta T,|\omega|) , \tag{7}$$

where β ranges from $\pi^2/8$ at the weak-coupling limit $\alpha\ll 1$ to $\pi/2$ for the hypothetical strong-coupling $\alpha\gg 1$ limit. Estimates of α from resistivity data of $YBa_2Cu_3O_7$ and recent photoemission results for $Bi_2Sr_2CaCu_2O_8$ (Ref. 7) yield values of intermediate coupling strengths $0.5<\alpha<1$.[6]

Physically, Fermi-surface nesting modifies the region of momentum space for the electron scattering that is compatible with the Pauli exclusion principle. Thus nested orbits will generally yield larger electron cross sections with the possibility of the above unconventional scattering rate that may be valid down to very low frequencies in the case of nearly perfect nesting.

Formally, the on-site Coulomb repulsion influences $\chi''(\mathbf{Q},\omega)$ as well as the self-energy as seen in the many-body diagrams shown in Fig. 2.

By comparison, a conventional Fermi liquid in three dimensions[8] will exhibit $\Sigma''_{\rm FL}\propto\omega^2$ and a Drude relaxation

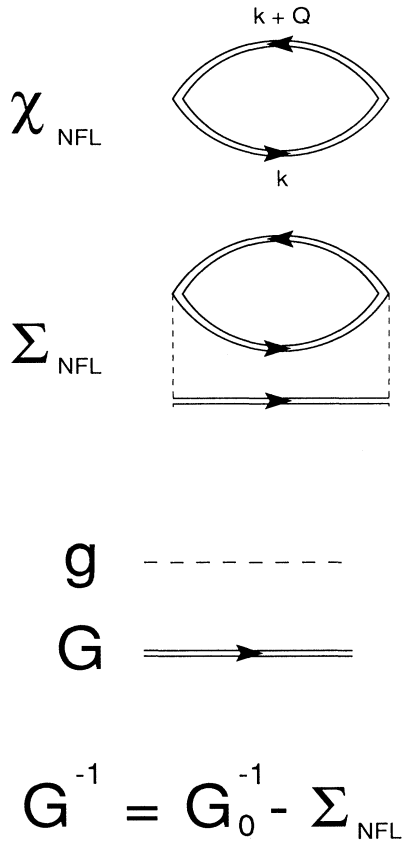

FIG. 2. Quasiparticle self-energy $\Sigma_{\rm NFL}$ and susceptibility $\chi_{\rm NFL}$ in the self-consistent treatment that is needed for intermediate coupling $\bar{g}=U/W\sim 1$ in the event of substantial nesting of the Fermi surface. The double lines refer to the dressed Green's function G, which includes the self-energy $\Sigma_{\rm NFL}$.

time $\tau_{\rm FL}$ given by[9]

$$\tau_{\rm FL}^{-1}=\frac{\pi\bar{g}^2}{2W}[(2\pi T)^2+\omega^2]\ . \tag{8}$$

Electrons confined to two dimensions with an effective-mass dispersion yield weak logarithmic corrections to the conventional FL behavior of Eq. (8).

A one-dimensional electron gas is exceptional because momentum conservation in the scattering process determines the energy of the scattering electron in terms of the allowed states of the target electron. Luttinger realized that this dimensionality constraint yields a quasiparticle damping linear in frequency ω. By comparison, his classic proof of the quadratic variation of the damping in three-dimensional systems relies on treating the energies of the scattering electrons as independent variables.[8]

Raman-scattering experiments on $YBa_2Cu_3O_7$ have shown unusual electronic contributions which also differ from conventional metal spectra.[10] The low-frequency region has been attributed to interband transitions,[11] but the origin of the strong electronic Raman spectrum that is relatively constant up to ~ 1 eV remains a mystery.

Previously, the anomalous Raman spectrum stimulated a phenomenological hypothesis[12] by Watanabe *et al.* and Varma *et al.*, who began with the empirical function $\chi''(\mathbf{q}\simeq 0,|\omega|<T)\propto N(0)\omega/T$ and $\chi''(\mathbf{q}\simeq 0,|\omega|>T)\propto N(0)\mathrm{sgn}(\omega)$, and then presumed $\chi''(\mathbf{q},\omega)$ independent of q to derive a self-energy Σ'' emanating from χ'' that is qualitatively similar to our NFL resulting in Eq. (7). Furthermore, they deduced the quasiparticle weight Z_k, which is found to vanish logarithmically at the Fermi surface at zero temperature, thus naming the situation a "marginal" Fermi liquid. Also, they calculated the conductivity in connection with infrared data and developed a correlation between the susceptibility and NMR, specific-heat, and thermal conductivity behaviors, as well as the observed linear temperature variation of the resistivity.

Fermi-surface nesting will not allow the quasiparticle strength $Z_{\rm NFL}(\omega)$ to vanish.[6] Furthermore, the form of the long-wavelength susceptibility in our NFL analysis differs from the "marginal FL" hypothesis, as we shall see below.

The derivation of the relaxation rate $\tau_{\rm NFL}$ and effective mass $m^*_{\rm NFL}$ that enter in the optical properties is presented in Sec. II. Application of these results to recent reflectivity data on copper oxide superconductors is in Sec. III, and the conclusions of our analysis are given in Sec. IV.

II. QUASIPARTICLE DAMPING AND EFFECTIVE MASS

In view of the evidence for the strong NFL self-energy corrections that increase linearly at higher frequencies, we are led to examine the density-density correlations functions at long wavelengths that are appropriate to the optical spectra. We analyze the self-energy and vertex corrections on the same footing by considering the processes shown diagrammatically in Fig. 3. The on-site Coulomb repulsion U is presumed to dominate the scattering, and the influence of Fermi-surface nesting described by a nesting wave vector $\mathbf{Q}$ enters in the vertex function $V(\mathbf{k},\mathbf{q},i\omega,i\nu)$ as well as in the self-energy Σ, which was determined earlier.[6]

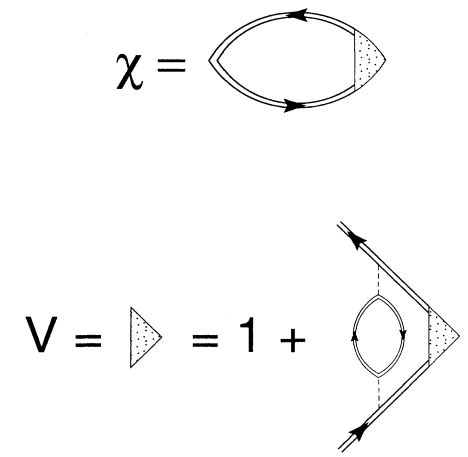

FIG. 3. Diagrams for the vertex corrections to the susceptiblity $\chi(\mathbf{q},i\nu)$. The vertex function $V(\mathbf{k},\mathbf{q},i\omega,i\nu)$ is represented by the shaded triangle.

A. Formalism

The basic interaction kernel is

$$K(\mathbf{q},i\nu)=g^2\chi_{\rm NFL}(\mathbf{q},i\nu)\ , \tag{9}$$

where the susceptibility $\chi_{\rm NFL}$ includes self-energy corrections as shown in Fig. 2. The "dressed" Green's function G is defined by

$$G^{-1}(\mathbf{k},i\omega)=i\omega-E(\mathbf{k})-\Sigma(\mathbf{k},i\omega)\ , \tag{10}$$

where the self-energy is determined by the self-consistent equation

$$\Sigma(\mathbf{k},i\omega)=\frac{1}{(2\pi)^3}\int d^3k'T\sum_{\omega'}K(\mathbf{k}-\mathbf{k}',i(\omega-\omega'))\times G(\mathbf{k}',i\omega')\ . \tag{11}$$

The corresponding self-energy graph is also in Fig. 2.

Including the vertex corrections as shown in Fig. 3 leads to the susceptibility

$$\chi(\mathbf{q},i\nu)=-\frac{1}{(2\pi)^3}\int d^3k\ T\sum_{\omega}G(\mathbf{k},i\omega)G(\mathbf{k}-\mathbf{q},i(\omega-\nu))\times V(\mathbf{k},\mathbf{q},i\omega,i\nu)\ , \tag{12}$$

and the integral equation for the vertex function becomes

$$V(\mathbf{k},\mathbf{q},i\omega,i\nu)=1+\frac{1}{(2\pi)^3}\int d^3k'T\sum_{\omega'}K(\mathbf{k}-\mathbf{k}',i(\omega-\omega')G(\mathbf{k}',i\omega')G(\mathbf{k}'-\mathbf{q},i(\omega-\nu))V(\mathbf{k}',\mathbf{q},i\omega',i\nu)\ . \tag{13}$$

B. Nesting approximation

The self-energy $\Sigma(\mathbf{k},i\omega)$ is evaluated at a momentum $\mathbf{k}$ that corresponds to a nested section of Fermi surface which is nearly parallel to the opposite section at $\mathbf{k}+\mathbf{Q}$. For the nested region of the orbit designated by the range of $\mathbf{k}$, backscattering processes are taken to be dominant because an explicit calculation[6] of $\chi''(\mathbf{Q},\omega)$ shows that this susceptibility is an order of magnitude larger than the conventional unnested Fermi-liquid response.

Presuming that the dominant contributions originate from wave vectors in the neighborhood of the nesting vector $\mathbf{Q}$, we neglect the momentum dependence of the kernel and thus use $K(\mathbf{q},i\nu)\simeq g^2\chi_{\rm NFL}(\mathbf{Q},i\nu)=K(i\nu)$. Then the self-energy reduces to

$$\Sigma(i\omega)=\frac{T}{(2\pi)^3}\sum_{\omega'}K(i(\omega-\omega'))\int d^3k'G(k',i\omega')\ . \tag{14}$$

Making the standard assumption of a density of states $N(\omega)\simeq N(0)$ to be constant close to the Fermi energy,

$$\begin{aligned}\Sigma(i\omega)&\simeq T\sum_{\omega'}K(i(\omega-\omega'))\int\frac{N(\xi)d\xi}{i\omega'-\xi-\Sigma(i\omega')}\\&=-i\pi TN(0)\sum_{\omega'}K(i(\omega-\omega'))\mathrm{sgn}(\omega')\end{aligned} \tag{15}$$

Hence we obtain

$$\Sigma(i\omega)=-i\,\mathrm{sgn}(\omega)\Gamma(i\omega)\ , \tag{16}$$

$$\Gamma(i\omega)=\pi N(0)T\sum_{|\nu|<|\omega|}K(i\nu)\ , \tag{17}$$

where we have presumed that $|\omega|$ and Γ are both much less than the bandwidth W. The simplified kernel allows the vertex to be treated as independent of momentum $\mathbf{k}$. Thus the vertex equation (13) simplifies to

$$\begin{aligned}V(\mathbf{q},i\omega,i\nu)=1+T\sum_{\omega'}&K(i(\omega-\omega'))F(\mathbf{q},i\omega',i\nu)\\&\times V(\mathbf{q},i\omega',i\nu)\ ,\end{aligned} \tag{18}$$

where

$$F(\mathbf{q},i\omega,i\nu)=\frac{1}{(2\pi)^3}\int d^3k\ G(\mathbf{k},i\omega)G(\mathbf{k}-\mathbf{q},i(\omega-\nu))\ . \tag{19}$$

C. Long-wavelength regime

Light couples to the excitations in the long-wavelength limit $qv_F\ll W$, where v_F is the Fermi velocity, and this limit allows a simple expansion of the energy denominator of the Green's function G in Eq. (19) to give

$$F(\mathbf{q},i\omega,i\nu)=N(0)\left\langle\frac{2\pi i\theta(0<\omega<\nu)}{i\nu+i[\Gamma(i\omega)+\Gamma(i\nu-i\omega)]-\mathbf{v}(\mathbf{k})\cdot\mathbf{q}}\right\rangle_{\rm FS}\ , \tag{20}$$

where $\nu\ll W$ is presumed and the Fermi-surface (FS) average is

$$N(0)\langle h(\mathbf{k})\rangle_{\rm FS}=\frac{1}{(2\pi)^3}\int d^3k\ \delta(E(\mathbf{k}))h(\mathbf{k})\ , \tag{21}$$

for a $\mathbf{k}$-dependent function h.

Now the vertex equation becomes

$$V(\mathbf{q},i\omega,i\nu)=1+2\pi iTN(0)\sum_{0<\omega'<\nu}V(\mathbf{q},i\omega',i\nu)\left\langle\frac{K(i(\omega-\omega'))}{i\nu+i[\Gamma(i\omega')+\Gamma(i\nu-i\omega')]-\mathbf{v}(\mathbf{k})\cdot\mathbf{q}}\right\rangle_{\rm FS}\ . \tag{22}$$

The susceptibility of Eq. (12) similarly reduces in the long-wavelength limit to

$$\chi(\mathbf{q},i\nu)=N(0)\left[1-2\pi iT\sum_{0<\omega<\nu}V(\mathbf{q},i\omega,i\nu)\left\langle\frac{1}{i\nu+i[\Gamma(i\omega)+\Gamma(i\nu-i\omega)]-\mathbf{q}\cdot\mathbf{v}(\mathbf{k})}\right\rangle_{\rm FS}\right]\ . \tag{23}$$

Performing the ω frequency summation with the limits $0<\omega<\nu$ in the vertex Eq. (22), and utilizing the identity

$$2\pi TN(0)\sum_{0<\omega'<\nu}K(i\omega-i\omega')=\Gamma(i\omega)+\Gamma(i\nu-i\omega)\ , \tag{24}$$

which follows from Eq. (17), yields the susceptibility in Eq. (23) in a more convenient form:

$$\chi(\mathbf{q},i\nu)=-\frac{2\pi N(0)\Gamma}{\nu}\sum_{0<\omega<\nu}\left\langle\frac{\mathbf{v}(\mathbf{k})\cdot\mathbf{q}}{i\nu+i[\Gamma(i\omega)+\Gamma(i\nu-i\omega)]-\mathbf{v}(\mathbf{k})\cdot\mathbf{q}}\right\rangle_{\rm FS}V(\mathbf{q},i\omega,i\nu)\ . \tag{25}$$

In the small-$\mathbf{q}$ limit, the expansion of the energy denominator readily shows that the leading-order susceptibility contribution in $\mathbf{q}$ is obtained by using the vertex $V(\mathbf{q}=0,i\omega,i\nu)$.

By inspection, the vertex solution

$$V(\mathbf{q}=0,i\omega,i\nu)=1+\frac{1}{\nu}[\Gamma(i\omega)+\Gamma(i\nu-i\omega)] \tag{26}$$

satisfies Eq. (22) for $\mathbf{q}=0$. Using the vertex of Eq. (26), we obtain a simplified relation for the long-wavelength susceptibility:

$$\chi(\mathbf{q}\simeq 0,i\nu)=-N(0)\langle[\mathbf{q}\cdot\mathbf{v}(\mathbf{k})]^2\rangle_{\mathrm{FS}}\frac{2\pi T}{\nu}\sum_{0<\omega<\nu}\frac{1}{i\nu\{i\nu+i[\Gamma(i\omega)+\Gamma(i\nu-i\omega)]\}}\ . \tag{27}$$

Finally, the frequency summation can be done to good accuracy by defining $\eta=[\Gamma(i\omega)+\Gamma(i\nu-i\omega)]/\nu$ and

$$\langle\eta\rangle=\frac{2\pi T}{\nu}\sum_{0<\omega<\nu}\eta(i\omega,i\nu)\ . \tag{28}$$

and then noting that

$$\left\langle\frac{1}{1+\eta}\right\rangle\simeq\frac{1}{1+\langle\eta\rangle}\left\langle\frac{1}{1+(\eta-\langle\eta\rangle)/(1+\langle\eta\rangle)}\right\rangle\simeq\frac{1}{1+\langle\eta\rangle}\left[1+O\left\langle\left[\frac{\eta-\langle\eta\rangle}{1+\langle\eta\rangle}\right]^2\right\rangle\right]\ , \tag{29}$$

providing that the deviation $(\eta-\langle\eta\rangle)/(1+\langle\eta\rangle)$ is small. This condition is shown to be satisfied for the NFL case in the next section. Thus we obtain

$$\chi(\mathbf{q}\simeq 0,i\nu)=\frac{-N(0)\langle[\mathbf{q}\cdot\mathbf{v}(\mathbf{k})]^2\rangle_{\mathrm{FS}}}{i\nu[i\nu+i\bar{\Gamma}(i\nu)]}\ , \tag{30}$$

where

$$\bar{\Gamma}(i\nu)=\frac{2\pi T}{\nu}\sum_{0<\omega<\nu}[\Gamma(i\omega)+\Gamma(i\nu-i\omega)]=\frac{4\pi T}{\nu}\sum_{0<\omega<\nu}\Gamma(i\omega)\ . \tag{31}$$

This form of $\chi(\mathbf{q}\simeq 0,i\nu)$ in Eq. (30) justifies the Drude expression of the dielectric function ϵ in Eq. (1).

D. NFL Damping

Fermi-surface nesting enhances the susceptibility at a nesting wave vector $\mathbf{Q}$. Presuming that this contribution dominates, we rewrite the basic kernel from Eq. (9) as

$$K_{\mathrm{NFL}}(i\nu)=\frac{g^2}{\pi}\int\frac{\chi''_{\mathrm{NFL}}(\mathbf{Q},\omega)}{\omega-i\nu}d\omega\ , \tag{32}$$

where the NFL susceptibility is in Eq. (5). Now the damping from Eq. (17) takes the form

$$\Gamma_{\mathrm{NFL}}(i\omega)=N(0)g^2T\int d\omega'\chi''_{\mathrm{NFL}}(\mathbf{Q},\omega')\sum_{|\nu|<|\omega|}\frac{1}{\omega'-i\nu}\ . \tag{33}$$

Using

$$T\sum_{|\nu|<|\omega|}\frac{1}{\omega'-i\nu}=\frac{1}{2}\coth\frac{\omega'}{2T}-\frac{1}{\pi}\mathrm{Im}\psi\left[\frac{1}{2}+\frac{|\omega|+i\omega'}{2\pi T}\right]\ , \tag{34}$$

where ψ is the diagamma function, Eq. (31) yields

$$\bar{\Gamma}_{\mathrm{NFL}}(i\nu)=N(0)g^2\int d\omega'\chi''_{\mathrm{NFL}}(\mathbf{Q},\omega')\left[\coth\left[\frac{\omega'}{2T}\right]-\frac{2}{\pi}\mathrm{Re}\left\{-i\psi\left[\frac{\nu+i\omega'}{2\pi T}\right]+\frac{\omega'}{\nu}\left[\psi\left[\frac{\nu+i\omega'}{2\pi T}\right]-\psi\left[\frac{i\omega'}{2\pi T}\right]\right]\right\}\right]\ , \tag{35}$$

which is analytic in the upper half-plane. Analytic continuation $i\nu\rightarrow\omega$ gives the NFL version of the Drude relaxation time τ_{NFL} defined by

$$\frac{1}{\tau_{\mathrm{NFL}}}=\mathrm{Re}\bar{\Gamma}_{\mathrm{NFL}}=N(0)g^2\int d\omega'\chi''_{\mathrm{NFL}}(\mathbf{Q},\omega')\left[\coth\left[\frac{\omega'}{2T}\right]-\coth\left[\frac{\omega'-\omega}{2T}\right]\right]\left[1-\frac{\omega'}{\omega}\right]\ . \tag{36}$$

We note here the important distinction between the quasiparticle damping Γ and the inverse transport lifetime $1/\tau$, which manifests itself in the appearance of different thermal factors in the expression for those quantities.[6,9]

In the special case of χ_{NFL} defined in Eq. (5), the quasiparticle damping from Eq. (33) can be shown to be of the form $\Gamma_{\mathrm{NFL}}(i\omega)\sim\omega\ln(\omega)$. If Γ is approximated to be linear in ω, the averaging procedure in Eq. (29) is exact. Therefore, the weak extra $\ln(\omega)$ dependence yields only a negligible correction, and the use of Eqs. (30) and (31) is justified.

The final result for the relaxation time follows from the NFL susceptibility given in Eqs. (5) and (6), which allows evaluation of the integral in Eq. (36) in the asymptotic limit $T\rightarrow 0$, which yields

$$\frac{1}{\tau_{\rm NFL}} = \alpha|\omega| \ , \tag{37}$$

and the static $\omega \to 0$ counterpart

$$\frac{1}{\tau_{\rm NFL}} = \frac{4\pi^2\alpha}{3\gamma} T \ . \tag{38}$$

Hence a reasonable representation of these results is

$$\frac{1}{\tau_{\rm NFL}} \simeq \alpha \max(\beta' T, |\omega|) \ , \tag{39}$$

where $\beta' = 4\pi^2/3\gamma$ varies from 3.3 in the weak-coupling limit $\alpha \ll 1$ to 4.2 in the strong-coupling case $\alpha \gg 1$. It is interesting to compare the crossover in the optical relaxation rate at $\omega = \beta' T$ with the corresponding crossover in the quasiparticle damping,[6] $\Gamma_{\rm NFL} = \alpha \max(\beta T, |\omega|)$, because the value of $\beta'/\beta = \frac{8}{3}$ is not far from the factor of 2 that appears in the optical response in the conventional Fermi-liquid result of Eq. (8).

It is interesting to notice that the static limit $\omega = 0$ yields $\Gamma_{\rm NFL}\tau_{\rm NFL} = \beta'/\beta' = \frac{3}{8}$, whereas the ordinary Fermi-liquid analysis predicts $\Gamma_{\rm FL}\tau_{\rm FL} = \frac{1}{4}$. However, in the higher-frequency regime $\omega \gtrsim T$, where the single-particle damping $\Gamma(\omega)$ can be measured (by photoemission for example), $\Gamma\tau = 1$ for nested as well as ordinary Fermi surfaces. Thus photoemission spectra and the optical reflectivity should give compatible damping estimates.

The unusual frequency variation of the Drude relaxation rate is shown in Fig. 4. The linear increase in $\tau_{\rm NFL}^{-1}$ at higher frequencies must terminate at a cutoff frequency which is at most $\omega_c = W/(1+\alpha)$.[6] Much weaker damping is evident in the standard FL result of Eq. (8) as seen in Fig. 4.

E. NFL Effective mass

Renormalization of the charge-carrier mass by electron-electron scattering is found by taking the Kramers-Kronig transform of the relaxation rate. This gives a Drude mass

$$\frac{m_D^*}{m_0} = 1 + \frac{2\alpha}{\pi} \ln \frac{\omega_c}{\max(\beta' T, |\omega|)} \ . \tag{40}$$

The frequency variation of the effective mass that enters in the optical properties is shown in Fig. 5 at two temperatures. As in the case of the optical relaxation rate $\tau_{\rm NFL}$, the frequency crossover in the Drude mass $m_D^*(T,\omega)$ occurs at $\omega = \beta' T$, whereas the real part of the quasiparticle self-energy exhibits a change near $\omega = \beta T$.[6] Experimental indications of a temperature- and a frequency-dependent Drude mass were noted earlier in the analysis of the optical conductivity of $YBa_2Cu_3O_x$.[3,5]

The apparent low-temperature divergence of the quasiparticle mass $m_{\rm NFL}^*$ raises doubts on the validity of a Fermi-liquid description. A quasiparticle at the Fermi surface will have a strength[6]

$$Z_{\rm NFL}(T=0) = \frac{1}{1 + (2\alpha/\pi)\ln(\omega_c/|\omega|)} \ , \tag{41}$$

which tends to vanish as $\omega \to 0$. This behavior was emphasized in the "marginal" Fermi-liquid phenomenological theory.[12]

If nesting is the source of the unusual self-energy

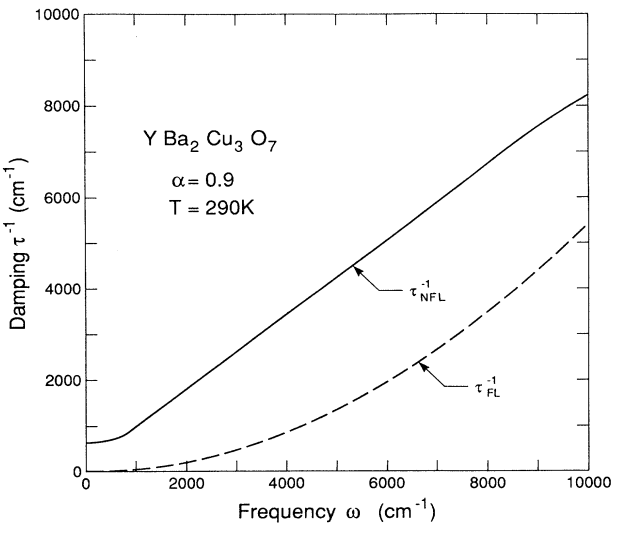

FIG. 4. Relaxation rates appropriate for the Drude dielectric function are shown by the solid curve for the NFL case using $\bar{g} \simeq 1.04$ and by the dashed curve for the ordinary Fermi-liquid result. At low frequencies $\omega < T$, the NFL behavior is $\tau_{\rm NFL}^{-1} = \alpha\beta T \simeq 3.52T$. The bandwidth was chosen as $W = 4$ eV, and both curves presume room temperature.

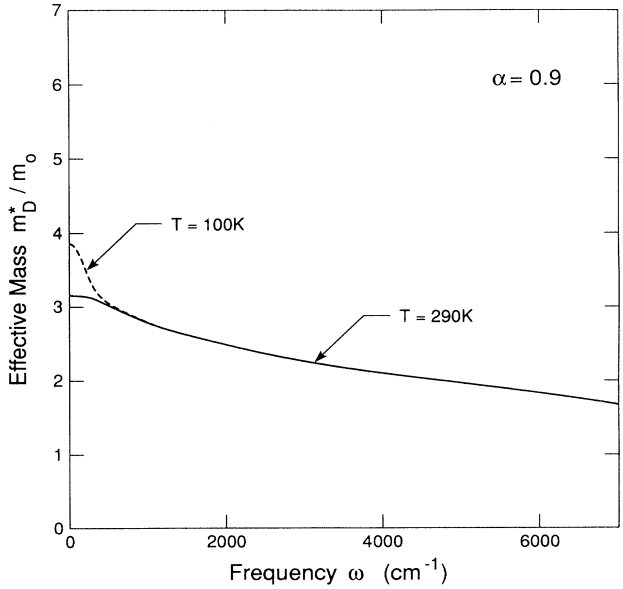

FIG. 5. Drude mass m_D^* from the NFL analysis is shown as a function of frequency at two temperatures for an intermediate Coulomb coupling $\bar{g} = 1.04$ and a cutoff frequency $\omega_c = 30\,000$ $\rm cm^{-1}$ ($\simeq 3.8$ eV).

features, then the quasiparticle strength will be prevented from vanishing by two plausible mechanisms. The likely occurrence of a phase transition to a spin-density wave (SDW), charge-density wave (CDW), or even superconducting state at a critical temperature T_c may be dictated by the specific nature of the nesting and the quasiparticle interactions, which may include an attractive component that is beyond the scope of the present work. Alternately, deviations from perfect nesting will correspond to a minimum temperature T^*, where our nesting approximations break down. Then, for $T<T^*$, the quasiparticle response will revert to conventional Fermi-liquid behavior at frequencies below T^*.

Evidence for nested Fermi surfaces has just been obtained by photoemission studies of $YBa_2Cu_3O_{6.9}$,[13] and the measured topology is in remarkably good agreement with results of band-structure calculations.[14,15]

III. REFLECTIVITY

The key results of the above analysis are represented by a modified Drude formula for the dielectric function

$$\epsilon_{\rm NFL}(\omega)=1-\frac{\omega_{\rm pl}^2}{\omega[(\omega/m_0)m_D^*+i/\tau_{\rm NFL}(\omega)]}\ , \tag{42}$$

where the frequency- and temperature-dependent mass m_D^* and relaxation time $\tau_{\rm NFL}$ are defined in Eqs. (40) and (39). In analyzing data we have as input the classical plasma frequency $\omega_{\rm pl}^2=4\pi e^2N(0)\langle[\mathbf{q}\cdot\mathbf{v}(\mathbf{k})/|\mathbf{q}|]^2\rangle_{\rm FS}$, the effective electron-electron coupling α defined in Eq. (6), and the cutoff frequency ω_c.

The reflectivity is given by

$$R(\omega)=\left|\frac{\epsilon^{1/2}-1}{\epsilon^{1/2}+1}\right|^2\ , \tag{43}$$

and thus a fit to optical data is feasible using Eq. (42) and (43).

We analyze the optical reflectivity of several copper oxide superconductors below. For convenience and clarity, we multiply the damping rate by a smooth function $(1+\omega^2/\omega_c^2)^{-1}$, which is insignificant at low frequencies and yet avoids unphysical structure that would appear near $\omega\sim\omega_c$ in a straightforward application of the damping formula. Also, we utilize a smooth interpolation formula

$$\max(\beta' T,\omega)=[(\beta' T)^2+\omega^2]^{1/2}\ , \tag{44}$$

which has the correct asymptotic behavior in line with Eq. (39). Thus formulas (39), (40), and (42)–(44) provide a simple convenient basis for analyzing the oxide data.

Since the unconventional quasilinear drop in the reflectivity as a function of frequency is a common feature of the cuprate superconductors, it is tempting to verify the comparable behavior of the NFL results analytically. In the wide frequency interval $T<\omega\ll\omega_{\rm pl}$, and $\omega<\omega_c$, the dielectric function reduces to the approximate form

$$\epsilon_{\rm NFL}(\omega)\simeq-\frac{\omega_{\rm pl}^2}{\omega^2}\frac{1}{m_D^*/m_0+i\alpha}\ , \tag{45}$$

and then the reflectivity reduces to the approximate function

$$R_{\rm NFL}(\omega)\simeq 1-\frac{2\sqrt{2}}{\omega_{\rm pl}}\left\{\left[\left[\frac{m_D^*}{m_0}\right]^2+\alpha^2\right]^{1/2}-\frac{m_D^*}{m_0}\right\}^{1/2}\ . \tag{46}$$

Considering the weak logarithmic frequency variation of m_d^* in the intermediate frequency range of interest (e.g., as seen in Fig. 5), it follows that a quasilinear drop in the reflectivity is in fact the expected qualitative behavior in the case of a nested Fermi surface.

At very low frequencies $\omega\leq T$, a more accurate representation of Eqs. (42)–(44) is needed, and the unusual temperature variation of the dielectric function may influence estimates of the superconducting energy gap from optical experiments.

We now proceed to analyze the reflectivity data of superconducting single crystals of $YBa_2Cu_3O_7$ and $Bi_2Sr_2CaCu_2O_8$. Then we examine the possibility of changing nesting conditions in $La_{2-x}Sr_xCuO_4$ in the metallic phase. Finally, we propose some predictions for the $Nd_{2-x}Ce_xCuO_4$ series of superconductors whose resistivity indicates a possible crossover to ordinary Fermi-liquid behavior at low temperatures.

A. $YBa_2Cu_3O_7$ and $Bi_2Sr_2CaCu_2O_8$

Optical reflectivity data[2] on a single crystal of $YBa_2Cu_3O_7$ with the polarization along the Cu-O plane is shown in Fig. 6 along with the NFL results using Eqs. (39)–(44). A remarkably good fit to the experiment is achieved using the parameters $\omega_{\rm pl}=16\,000$ cm^{-1} (2 eV) and $\alpha=0.9$, which corresponds to intermediate-strength Coulomb coupling $\bar{g}\simeq 1$. The overall structure of the reflectivity $R(\omega)$ in the frequency range shown in Fig. 6 is not very sensitive to the cutoff parameter taken as $\omega_c=30\,000$ cm^{-1}.

The estimate of intermediate coupling $\alpha\simeq 0.9$ is compatible with the resistivity data as well. A crude estimate yields the dc resistivity $\rho\simeq 4\pi\alpha\beta' T/\omega_{\rm pl}^2\simeq 165$ $\mu\Omega$ cm at room temperature, and this value is in the ballpark of the measured reflectivity of the high-purity crystals analyzed by Watanabe *et al.*[2]

It is interesting to note that the data[3] of Collins *et al.* on untwinned crystals shown in Fig. 1 yields a similar quasilinear drop in the reflectivity over the frequency range 0.1 eV $<\omega<$ 1 eV. The raw reflectivity data is surprisingly similar for the electric field parallel to the Cu-O chains and the perpendicular polarization over the energy range shown in Fig. 1.

A quite similar variation of the reflectivity is seen[16] for $Bi_2Sr_2CaCu_2O_8$ in Fig. 6, and accordingly only a change in the plasma frequency to $\omega_{\rm pl}=1.4$ eV is sufficient to yield a good correspondence to the NFL theoretical curve. It is interesting that the slope of $R(\omega)$ for $Bi_2Sr_2CaCu_2O_8$ is steeper than the $YBa_2Cu_3O_7$ data. The interpretation of this difference in terms of a simple change in the plasma frequency is not unique, since the coupling $\alpha=0.9$ was held constant. A large increase in the coupling beyond the intermediate strength range

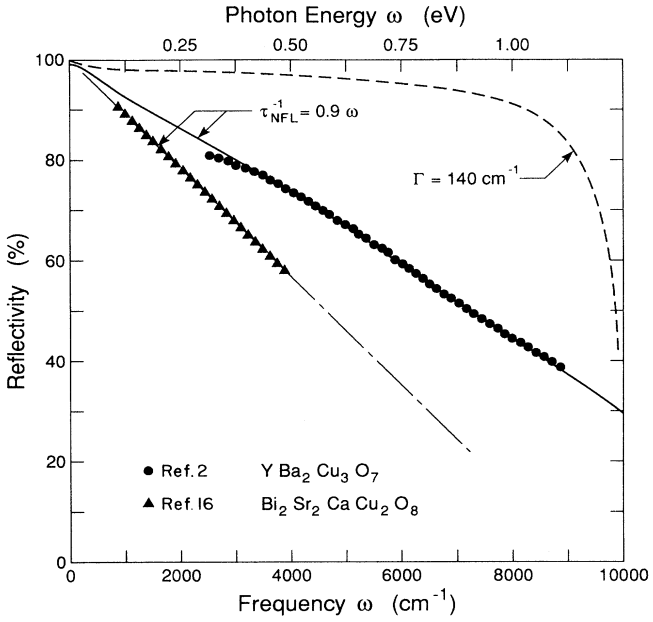

FIG. 6. Relectivity data for $YBa_2Cu_3O_7$ (Ref. 2) and $Bi_2Sr_2CaCu_2O_8$ (Ref. 16) compared to the NFL theory result using an intermediate strength Coulomb coupling $\bar{g}=1.04$ for both curves. The solid curve shows the calculated reflectivity using a plasma frequency $\omega_{pl}=16000\ cm^{-1}$ (2 eV) for $YBa_2Cu_3O_7$. The dot-dashed curve yields a good fit to $Bi_2Sr_2CaCu_2O_8$ using $\omega_{pl}=1.4$ eV with the approximate $R(\omega)$ formula of Eq. (46). By contrast, the conventional Drude behavior for a constant damping term Γ gives the dashed curve.

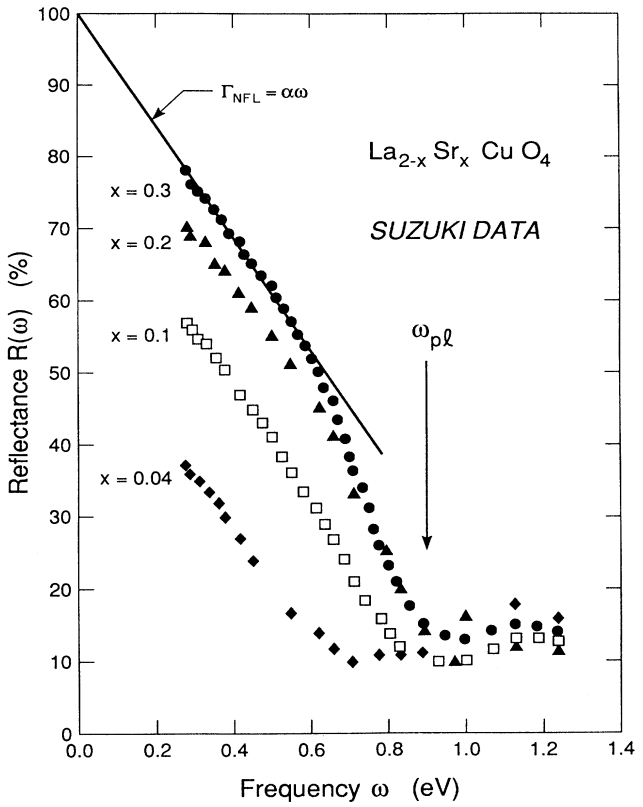

FIG. 7. Raw reflectivity data for $La_{2-x}Sr_xCuO_4$ single-crystal films from Ref. 18 is shown at various compositions. The plasma "dip" is indicated near 0.85 eV. In common with other copper oxide superconductors, the metallic response for $x=0.3$ follows the quasilinear drop in frequency, which is well described by the calculated curve using $\alpha=0.5$. At smaller Sr content, the reflectivity data does not extrapolate at 100% in the zero-frequency limit, and this may indicate inhomogeneities in the sample surfaces.

$\alpha \simeq 1$ would require the consideration of higher-order corrections in the NFL theory.[6]

Alternate fits with ordinary Drude model parameters are subject to the difficulty demonstrated by the dashed curve in Fig. 6, which was obtained with a commonly used small and constant damping such as $\Gamma=140\ cm^{-1}$ and a plasma frequency $\omega_{pl}=9600\ cm^{-1}$ (1.2 eV): Clearly, the resulting conventional Drude reflectivity is far from experiment. Choosing a huge damping $\Gamma=1600\ cm^{-1}$ also fails[2] to reproduce the data. These discrepancies have led to a variety of models of midinfrared oscillator contributions which require arrays of additional parameters.[2-5]

Changes in chemical composition are expected to modify the nesting features of the Fermi surface, and the resulting optical features may further distinguish the NFL predictions from ordinary Drude behavior. An example of this situation is considered next.

B. $La_{2-x}Sr_xCuO_4$

The magnetic properties of the insulating host compound La_2CuO_4 have stimulated various novel ideas for superconductivity mechanisms. Furthermore, the discovery[17] of a large positive Hall coefficient R_H at small Sr context $x \simeq 0.05$ led to the commonly held view that a small number holes induced by Sr doping provide the charge carriers essential to the electrical transport. Hall data on single-crystal films[18] showed a strong temperature variation of $R_H(T,x)$ and values at $x \sim 0.3$ that were orders of magnitude smaller than the naive $1/x$ behavior expected for a doped semiconductor.

By contrast, reflectivity data[18,19] on metallic samples with $x > 0.06$ fail to conform to the notion of a plasma frequency that might be expected to vary as $\omega_{pl} \sim x^{1/2}$ in the simple doping picture. Instead, optical experiments on single-crystal films reveal a "dip" in the reflectivity that indicates the surprising feature of a plasma frequency that is roughly constant over a wide Sr range $0.05 \leq x < 0.4$.

Band-structure computations[20] suggest a nearly constant plasma frequency in $La_{2-x}Sr_xCuO_4$, because the dominant contribution to the dielectric response comes from the nearly half-filled Cu $d_{x^2-y^2}$ band. However, these band results neglect the on-site Coulomb repulsion and incorrectly predict a metallic state at $x=0$. Furthermore, they yield a Hall coefficient unlike the observed

values in the metallic region.

A reconciliation of the apparent conflicts in the Hal effect, band-structure results, and optical evidence for the plasma frequency has been proposed[21] from calculations of the electron mobility caused by electron-electron scattering in a simple nearly half-filled tight-binding energy band in two dimensions. The key point is that the electron mobility becomes very small close to half-filling and its approach to zero signals a metal-insulator transition at $x \simeq 0.06$ Providing that the Fermi energy E_F intersects a narrow band of hole states as well, the more mobile holes dominate the Hall effect at low concentrations. At intermediate Sr content, $0.06 < x < 0.4$, the many-body effects yield[21] the observed decrease of the Hall coefficient by orders of magnitude as the electron mobility increases and yet maintain a nearly constant plasma frequency corresponding to the total contributions of the majority electrons and minority holes. The electron orbits in the tight-binding model exhibit nesting which is sensitive to the placement of the Fermi energy as a function of Sr doping. Thus the spectral shape of the reflectivity $R(\omega)$ is expected to vary as the scattering rate changes, even though the plasma frequency may remain nearly constant.

A straightforward analysis of the raw reflectivity data[18] on $La_{1.7}Sr_{0.3}CuO_4$ single-crystal films in Fig. 7 shows the same quasilinear decrease in $R(\omega)$ up to $\omega \sim 0.7$ eV. This range is well represented by Eqs. (39)–(44) with a coupling constant $\alpha = 0.5$ and a plasma frequency $\omega_{\rm pl} \simeq 1$ eV. At higher frequencies the reflectivity drops to a minimum near 0.9 eV and then saturates to roughly 15%.

Lower Sr composition samples are expected to have inhomogeneities which complicate the optical properties. Evident flaws in the measured raw data for $x < 0.2$ in Fig. 7 are the extrapolations at $\omega = 0$, which are well below the ideal 100% reflectivity. Nevertheless, the reflectivity dip is consistently close to 0.9 eV for $x = 0.1$, 0,2, 0.3. To surmount the obstacle of inhomogeneous regions, we follow a simple data-reduction procedure suggested to us by S. E. Schnatterly (private communication). We express the total reflectivity as

$$R_{\rm expt} = fR_I + (1-f)R_m(\omega) , \tag{47}$$

where the metallic part R_m of Eqs. (39)–(44) is reduced by a consant fraction $1-f$. The remaining fraction f of the sample that deviates from perfect structural stoichiometry is represented by a constant reflectivity R_I. For simplicity, we take $R_I \simeq 0.2$ and use Eq. (47) to unravel the metallic R_m contribution shown in Fig. 8. The value of $f(x)$ is determined by the condition $R_m(\omega = 0) = 100\%$. The reduced reflectivity shows the quasilinear decrease as a function of frequency in line with the other superconducting oxides examined above. The variation in the slope of the $R(\omega)$ versus ω curves is compatible with our NFL analysis as shown by the theoretical cuves in Fig. 8. However, the variation of the parameters α and $\omega_{\rm pl}$ with Sr content is difficult to pinpoint. A good fit to the data is achieved with a constant plasma frequency $\omega_{\rm pl} = 1$ eV and then allowing the interaction parameter α to decrease with increasing Sr content. This view is compatible with the two-dimensional (2D) tight-binding model[21] which would yield more nested regions of the Fermi surface at the lower Sr content and hence a larger damping $\tau_{\rm NFL}^{-1} \simeq \alpha\omega$ from Eq. (39). On the other hand, the slope of $R(\omega)$ is also sensitive to the choice of the plasma frequency $\omega_{\rm pl}$, so that quantitative comparisons of the α and $\omega_{\rm pl}$ parameters are not rigorous.

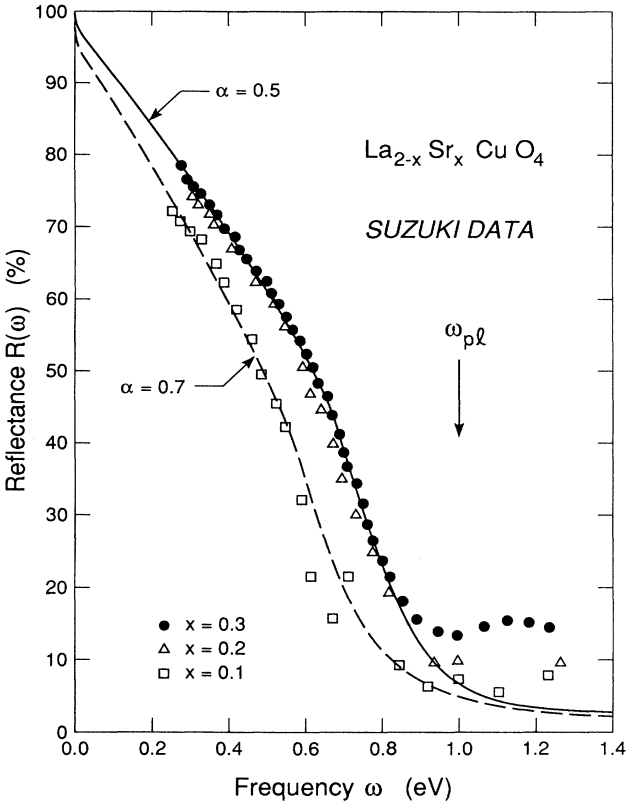

FIG. 8. Reduced data for the metallic contribution $R_m(\omega)$ to the reflectivity of $La_{2-x}Sr_xCuO_4$ extracted from Eq. (47). The nonmetallic contribution was taken as $R_I \simeq 0.2$ for all three curves, and the nonmetallic fractions are $f(x=0.3)=0$, $f(x=0.2)=0.11$, and $f(x=0.1)=0.29$. These fractions are chosen so that $R_m(\omega)$ extrapolates to 100% at $\omega = 0$. The corresponding NFL theory curves use a plasma frequency $\omega_{\rm pl} = 1$ eV and an intermediate value of the Coulomb coupling $\bar{g} = 0.67$ for $x = 0.3$ and for $x = 0.2$, and $\bar{g} = 0.85$ for $x = 0.1$

It should be noted that the lowest-concentration sample $La_{1.96}Sr_{0.04}CuO_4$ has a much larger resistivity[18] and much lower reflectivity as seen in the raw data of Fig. 7. Hence the determination of the metallic components $R_m(\omega)$ using Eq. (47) is especially prone to uncertainties near the metal-insulator transition.

C. $Nd_{2-x}Ce_xCuO_4$

The cuprates in this category are often called n-type superconductors since early Hall data showed dominant electron contributions. They provide additional puzzles

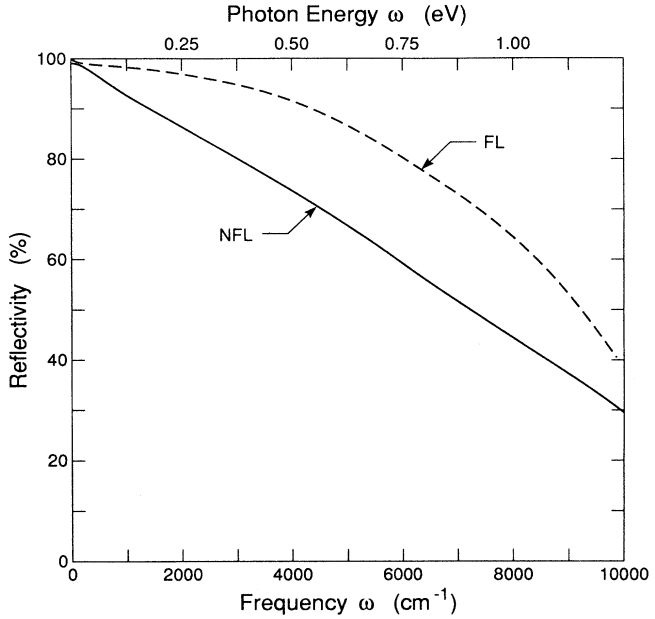

FIG. 9. Comparison of the conventional Fermi-liquid prediction for the reflectivity $R_{\rm FL}(\omega)$ and the NFL analysis with a linear frequency variation to the damping. Both curves are computed using intermediate Coulomb coupling $\bar{g}=1.04$, a bandwidth $W=4$ eV, and $\omega_{\rm pl}=2$ eV. These results are at room temperature.

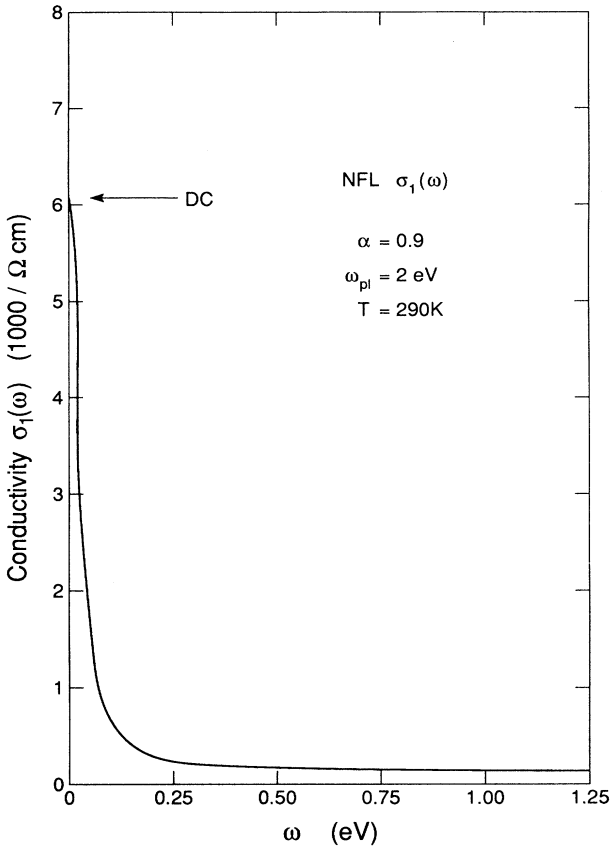

FIG. 10. Optical conductivity as a function of frequency is shown for a system with Fermi-surface nesting at $T=290$ K. The parameters $\bar{g}=1.04$, $\omega_{\rm pl}=2.0$ eV correspond to the values deduced from the reflectivity data of $YBa_2Cu_3O_7$. The midinfrared ω^{-1} "tail" in the conductivity is an intrinsic feature of our NFL analysis.

for theory by exhibiting an unusual resistivity which appears to follow the conventional FL behavior of $\rho \propto T^2$ at low temperatures and then $\rho \propto T$ at temperatures in excess of a crossover $T^* \sim 100$ K.[22,23] The strange $\rho(T)$ behavior is extremely sensitive to sample preparation and composition, and very careful fits demonstrate the validity of 2D Fermi-liquid calculations at low temperatures.[24]

Optical measurements should reveal the extent of the Fermi-liquid behavior as shown in Fig. 9 for the Drude model with the ordinary damping $\tau_{\rm FL}^{-1}$ of Eq. (8). By contrast, the idealized nested Fermi-surface reflectivity is shown by the solid curve. Using the crossover in the measured resistivity as a guide, we may infer a crossover temperaure T^*, which is proportional to the deviation from perfect nesting, so that below T^* the FL behavior is valid for the reflectivity below a corresponding value of frequency $\omega^* \simeq 4T^*$, where $\tau_{\rm FL}^{-1}(\omega<\omega^*) \propto \omega^2$ as in Eq. (8), while $\tau^{-1} \propto \omega$ for $\omega > \omega^*$. On the other hand, for temperatures $T > T^*$, where a linear resistivity variation is seen, the NFL analysis would predict $\tau_{\rm NFL}^{-1}(\omega) \simeq \alpha \max(\beta' T, \omega)$ with a corresponding quasilinear drop in the reflectivity. This relation between the dc electrical transport and the higher-frequency optical response may be interesting to probe experimentally.

IV. CONDUCTIVITY

The frequency variation of the real part of the conductivity from Eq. (3) develops a high-frequency component as a result of Fermi-surface nesting. Using the NFL damping and Drude mass m_D^* from Eqs. (39) and (40), we obtain

$$\sigma_{1,\rm NFL}(\omega)=\frac{\omega_{\rm pl}^2}{4\pi\tau_{\rm NFL}}\left[\omega^2\left[\frac{m_D^*}{m_0}\right]^2+\frac{1}{\tau_{\rm NFL}^2}\right]^{-1} . \quad (48)$$

As seen in Fig. 10, the low-frequency part of the conductivity has a sharp peak reaching the dc limit

$$\sigma_{1,\rm NFL}(\omega=0)=\omega_{\rm pl}^2/(4\pi\alpha\beta' T) . \quad (49)$$

This region is qualitatively similar to the usual Drude behavior for $\omega \leq T$. However, the enhanced damping rate $\tau_{\rm NFL}^{-1}(\omega)=\alpha\omega$ yields the unconventional ω^{-1} higher-frequency "tail" extending the $\omega \sim 0.5$ eV in Fig. 10. By contrast, the usual Drude conductivity falls off as ω^{-2}.

Previous analysis of the superconducting cuprates were troubled by the experimental spectral weight in the midinfrared range 0.1 eV $<\omega<$ 1 eV. Our NFL analysis provides an alternate interpretation of the midinfrared region based on electron-electron scatterng and damping. The physical origin of the midinfrared absorption is

clearly important in estimates of the carrier density from the f-sum rule for example, since the tail region is an intrinsic part of $\sigma_{1,\mathrm{NFL}}(\omega)$.

V. RAMAN SCATTERING AND ELECTRON-LOSS SPECTRUM

Inelastic light scattering by electron-hole excitations from a single band is expected to be weak by virtue of a small cross section.[11] Nonetheless, it is interesting to explore the modifications in the long-wavelength structure of the Raman spectrum in the nested Fermi orbit case.

The first-order Raman intensity is given by

$$I(\omega)=\frac{d^2\sigma}{d\omega\, d\Omega}=\hbar\left[\frac{\omega_I}{\omega_S}\right]^2\left[\frac{e^2}{mc^2}\right]^2 \times\frac{(\mathbf{e}_I\cdot\mathbf{e}_S)^2\chi''(\mathbf{q},\omega)}{1-\exp(-\omega/T)}\ , \tag{50}$$

where the incoming light with momentum $\mathbf{k}_I$ and frequency ω_I is scattered to a final state with $\mathbf{k}_S$ and ω_S by an excitation with $\mathbf{q}=\mathbf{k}_I-\mathbf{k}_S$ and $\omega=\omega_I-\omega_S$. Hence the frequency variation for $I(\omega)$ is determined by the imaginary part of the susceptibility $\chi''(\mathbf{q},\omega)$ at small momenta $\mathbf{q}\simeq 0$. Normal free electrons yield a susceptibility in this regime that exhibits a peak near $qv_F\simeq 100\ \mathrm{cm}^{-1}$.

Electron-loss spectroscopy also measures $S(\mathbf{q},\omega)\sim\chi''(\mathbf{q},\omega)$, and the data[25] on $Bi_2Sr_2CaCu_2O_8$ provides a striking confirmation of the line shape at small $q=0.05$ Å^{-1} predicted by Eq. (42) with the same electron-electron scattering $\alpha=0.9$, as used in the reflectivity, and a plasma frequency of $\omega_{\mathrm{pl}}=1.45$ eV, which yields the electron-loss peak by comparison to the $\omega_{\mathrm{pl}}=1.4$ eV that we inferred from the reflectivity analysis.

The discovery[10] of a large electronic contributon in the Raman spectrum of the cuprate superconductors stimulated various theoretical suggestions. The puzzling behavior at low frequencies has been attributed to interband transitions.[11] However, the nearly constant spectral strength extending up to $\omega\sim 0.5$ has remained a mystery. In fact, the anomalous Raman spectrum was the starting input for the empirical susceptibility $\chi''(\mathbf{q}\simeq 0,\omega)$ used in the marginal Fermi-liquid theory.[12]

The first-order Raman spectrum from the NFL analysis differs from the data in a significant way when both self-energy and vertex corrections are included in the analysis which led to the dielectric function $\epsilon_{\mathrm{NFL}}(\omega)$ in Eq. (42). A straightforward generalization of the Raman formula of Eq. (50) yields $I(\omega)\propto \mathrm{Im}\epsilon^{-1}_{\mathrm{NFL}}(\omega)$, and this function predicts a smoothly increasing intensity with frequency up to nearly the plasma frequency. Hence the main influence of nesting is a broadening of the plasmon spectra line shape.

In view of the nearly constant observed spectrum, and the anomalous frequency and temperature variation of the susceptibility $\chi''_{\mathrm{NFL}}(\mathbf{Q},\omega)$ in Eq. (5), it may be worthwhile to consider second-order processes. Such a process should be compatible with the observed selection rules and overall magnitude of the scattering. In this connection the evolution[26] of the two-magnon Raman spectrum in the insulating cuprates to the electronic contribution in the metallic phases provides important clues to the origin of the anomalous electronic processes in the superconductors.

VI. CONCLUSIONS

The anomalous quasilinear decrease of the reflectivity observed in several copper oxide superconductors has been explained in terms of an unusual frequency dependence in the relaxation time and the effective mass of the charge carriers. The physical origin of the damping is attributed to electron-electron scattering within a simple model which includes the on-site Coulomb repulsion U and modification in the response caused by Fermi-surface nesting. Analysis of reflectivity data for $YBa_2Cu_3O_7$, $Bi_2Sr_2CaCu_2O_8$, and $La_{2-x}Sr_xCuO_4$ indicates intermediate coupling strengths with U comparable to the bandwidth W.

Although nested orbits yield an anomalous temperature and frequency variation to the susceptibility at the nesting wave vector $\mathbf{Q}$, the long-wavelength susceptibility in the NFL analysis is much smaller in magnitude over a wide frequency range $\omega>T$. At small momenta appropriate to the optical response, the NFL susceptibility and dielectric function appear in a Drude form with the relaxation rate $\tau^{-1}_{\mathrm{NFL}}(T,\omega)$, showing a linear frequency variation for $\omega>T$ and an effective mass $m^*_D(T,\omega)$ that is weakly dependent on frequency.

The nested Fermi-liquid formulas yield a simple interpretation of optical reflectivity in terms of the conventional plasma frequency ω_{pl} and an effective electron-electron coupling $\bar{g}=U/W$, without recourse to additional parameters for the midinfrared region. However, unique estimates of the coupling $\bar{g}$ would require an indepenent determination of the plasma frequency or vice versa. Thus electron-loss and photoemission spectroscopy may help to pin down quantitative estimates of the charge-carrier density in the high-temperature superconductors.

Electronic structure with perfect nesting exhibits several analogies with 1D systems, including the linear frequency variation of the damping and linear T dependence of the resistivity.[27] Hence the higher-order many-body effects[28] that yield important corrections in 1D should be examined more thoroughly in nested examples with higher dimensionality. The quasiparticle strength $Z_{\mathrm{NFL}}(\omega)$ will not vanish at zero frequency, however, because a phase transition to a CDW, SDW, or perhaps superconducting phase should occur at a finite temperature. The instability[29] toward a phase transition depends on details of the Fermi-surface nesting and the nature of the quasiparticle interactions. The photoemission evidence for the existence of a Fermi surface is compatible with our result of a finite quasiparticle strength at the Fermi surface, even in the event of a partially nested Fermi surface of the type recently revealed $YBa_2Cu_3O_{6.9}$.[13] As the temperature is lowered for the imperfect nesting case, the NFL behavior for the damping may revert to ordinary Fermi-liquid result below a crossover temperature T^*, providing, of course, that T^* exceeds the phase transition

temperature. Evidence for such an unusual crossover appears in the resistivity variation of $Nd_{2-x}Ce_xCuO_4$, and it would be interesting to test the theoretical prediction of a corresponding frequency crossover in the reflectivity of these samples.

Raman scattering by itinerant electron-hole pairs is expected to be weak in first order where the light cross secton is proportional to the long-wavelength susceptibility. Our results for $\chi''(\mathbf{q}\simeq 0,\omega)$ confirm weak first-order scattering when both self-energy and vertex corrections are included.Thus nesting yields a susceptibility whose frequency variation and magnitude are much different at $\mathbf{q}\simeq 0$ than at the nesting wave vector $\mathbf{Q}$. This feature of the NFL theory is in contrast to the phenomenological hypothesis of the marginal Fermi-liquid theory.[12]

Nesting introduces a novel behavior to the susceptibility that is relatively model independent. Following the suggestion of Dzyaloshinki,[29] the frequency variation of $\chi''(\mathbf{Q},\omega)$ is apparent from the fluctuation dissipation theorem which relates the susceptibility to the mean-square density fluctuation component $\langle \rho_q^+, \rho_q \rangle_\omega$. Quasistatic fluctuations at a characteristic momentum $\mathbf{q}\simeq\mathbf{Q}$ yield the general shape of the $\chi''_{\mathrm{NFL}}(\mathbf{Q},\omega)$ as a function of temperature and frequency, and this observation also clarifies the origin of the exceptional response at a particular momentum $\mathbf{Q}$, while the long-wavelength behavior is quite different.

Second-order Raman scattering may probe contributions from large momenta $\sim\mathbf{Q}$. The NFL results for the susceptibility indicate a large cross section for this process, and the nearly constant $\chi''_{\mathrm{NFL}}(\mathbf{Q},\omega)$ up to large frequencies $T<\omega<\omega_c$ may provide an explanation for the observed anomalous electronic Raman spectrum in the copper oxide superconductors.

Is nesting a key ingredient for high-temperature superconductivity? The evidently ubiquitous reflectivity variation among the cuprates is amazing, but the observation of similar behavior[2] in the low-temperature superconductor $Bi_2Sr_2CuO_{6+\delta}$ suggests that the quasilinear drop in $R(\omega)$ is not a sufficient condition. From the theoretical point of view, the instability of one-dimensional systems toward formation of spin density waves in competition with superconducting pairing of electrons or holes provides many issues[28–31] that warrant future study in two-dimensional structures with nested Fermi surfaces.

Note added in proof. The self-energy and vertex corrections satisfy the Ward identity required for gauge invariance and charge conservation as discussed, for example, in *Superconductivity,* by J. R. Schrieffer (Benjamin, New York, 1964), Chap. 8. The proof follows from Eqs. (16) and (26), or alternately from a term by term inspection of the diagrams for the self-energy and vertex in Figs. 2 and 3. In cases where the system is close to a spin-wave instability, other contributions become important, including the ladder series of electron-hole bubbles that dress the self-energy and the corresponding vertex terms that are needed for a conserving approximation. The latter graphs are analogous to "phonon-drag" contributions in the case of electron-phonon coupling.

ACKNOWLEDGMENTS

We appreciate very constructive comments by I. E. Dzyaloshinki, S. E. Schnatterly, and C. C. Tsuei, and we thank Z. Schlesinger for providing infrared data on untwinned crystals prior to publication. We have enjoyed stimulating discussions with E. Abrahams, M. V. Klein, N. P. Ong, and A. Zawadowski. This research is supported by the U. S. Department of Energy Grant NO. DEF 605-84-ER 45113.

*Permanent address: Central Research Institute for Physics, 1525 Budapest 114, P.O. Box 49, Hungary.

[1]R. E. Glover III and M. Tinkham, Phys. Rev. **108**, 243 (1957).

[2]Y. Watanabe, Z. Z. Wang, S. A. Lyon, D. C. Tsui, N. P. Ong, J. M. Tarascon, and P. Barboux, Phys. Rev. B **40**, 6884 (1989).

[3]R. T. Collins, Z. Schlesinger, F. Holtzberg, P. Chaudhari, and C. Feild, Phys. Rev. B **39**, 6571 (1989). The untwinned sample studies are by Z. Schlesinger *et al.*, Phys. Rev. Lett. **65**, 801 (1990).

[4]K. Kamaras, K. L. Herr, C. D. Porter, N. Tache, D. B. Tanner, S. Etemad, T. Venkatesan, E. Chase, A. Inam, X. D. Wu, M. S. Hegde, and B. Dutta, Phys. Rev. Lett. **64**, 84 (1990).

[5]G. A. Thomas, J. Orenstein, D. H. Rapkine, M. Capizzi, A. J. Millis, R. H. Bhatt, L. F. Schneemyer, and J. Wasczak, Phys. Rev. Lett. **61**, 1313 (1988).

[6]A. Virosztek and J. Ruvalds, Phys. Rev. B **42**, 4064 (1990).

[7]C. G. Olson, R. Liu, D. W. Lynch, R. S. List, A. J. Arko, B. W. Veal, Y. C. Chang, P. Z. Jiang, and A. P. Paulikas, Phys. Rev. B **42**, 381 (1990).

[8]J. M. Luttinger, Phys. Rev. **121**, 942 (1961). A general textbook discussion is in D. Pines and P. Nozieres, *The Theory of Quantum Liquids* (Benjamin, New York, 1966).

[9]R. N. Gurzhi, Zh. Eksp. Teor. Fiz. **35**, 965 (1958) [Sov. Phys. —JETP **8**, 673 (1959)].

[10]S. L. Cooper, F. Slakey, M. V. Klein, J. P. Rice, E. D. Bukowski, and D. M. Ginsberg, Phys. Rev. B **38**, 11934 (1988), F. Slakey, S. L. Cooper, M. V. Klein, J. P. Rice, and D. M. Ginsberg, *ibid.* **39**, 2781 (1989).

[11]H. Monien and A. Zawadowski, Phys. Rev. Lett. **63**, 911 (1989).

[12]C. M. Varma, P. B. Littlewood, S. Schmitt-Rink, E. Abrahams, and A. E. Ruckenstein, Phys. Rev. Lett. **63**, 1996 (1989).

[13]J. C. Campuzano, G. Jennings, M. Faiz, L. Beaulaigue, B. W. Veal, J. Z. Liu, A. P. Paulikas, K. Vandervoort, H. Claus, R. S. List, A. J. Arko, and R. J. Bartlett, Phys. Rev. Lett. **64**, 2308 (1990).

[14]L. F. Mattheiss, Phys. Rev. Lett. **58**, 1028 (1987).

[15]J. Yu, A. J. Freeman and J. H. Xu, Phys. Rev. Lett. **58**, 1035 (1987).

[16]J. H. Kim, I. Bozivic, D. B. Mitzi, A. Kapitulnik, and J. S. Harris, Jr., Phys. Rev. B **41**, 7251 (1990).

[17]N. P. Ong, Z. Z. Wang, J. Clayhold, J. M. Tarascon, L. H. Green, and W. R. McKinnon, Phys. Rev. B **35**, 8807 (1987).

[18]M. Suzuki, Phys. Rev. B **39**, 2312 (1989).
[19]S. Tajima, S. Uchida, S. Tanaka, S. Kanbe, K. Kitazawa, and K. Fueki, Jpn. J. Appl. Phys. **26**, L432 (1987).
[20]P. B. Allen, W. E. Pickett, and H. Krakauer, Phys. Rev. B **36**, 3926 (1987).
[21]J. Ruvalds and A. Virosztek, Phys. Rev. B **42**, 399 (1990).
[22]J. M. Tarascon, E. Wang, L. H. Greene, B. G. Bagley, G. W. Hull, S. M. De'Egidio, P. F. Miceli, Z. Z. Wang, T. W. Jing, J. Clayhold, D. Brawner, and N. P. Ong, Phys. Rev. B **40**, 4494 (1989).
[23]Y. Hidaka and M. Suzuki, Nature **338**, 635 (1989).
[24]C. C. Tsuei, A. Gupta, and G. Koren, Physica C **161**, 415 (1989).
[25]N. Nücker, H. Romberg, S. Nakai, B. Scheerer, J. Fink, Y. F. Yan, and Z. X. Zhao, Phys. Rev. B **39**, 12379 (1989).
[26]K. B. Lyons and P. A. Fleury, J. Appl. Phys. **64**, 6075 (1988).
[27]L. P. Gorkov and I. E. Dzyaloshinki, Pis'ma Zh. Eksp. Teor. Fiz. **18**, 686 (1973).
[28]J. Solyom, Adv. Phys. **28**, 201 (1979).
[29]I. E. Dzyaloshinki, Zh. Eksp. Teor. Fiz. **93**, 1487 (1987) [Sov. Phys.—JETP **66**, 848 (1987)].
[30]V. J. Emery, in *Highly Conducting One-Dimensional Solids,* edited by J. T. Devreese, E. P. Evrard, and V. E. Van Doren (Plenum, New York, 1979), p. 247.
[31]H. Gurtfreund and W. A. Little, in *Highly Conducting One-Dimensional Solids,* edited by J. T. Devreese, E. P. Evrard and V. E. Van Doren (Plenum, New York, 1979), p. 305.